

Coal Pillar Width Design in High-stress Gob-side Entry Driving

Lifeng Li^{1,2,3}, Weili Gong^{1,2}, Jiong Wang^{1,2*}, Huilin Deng^{1,3}, Qianqian Jiang^{1,2} and Yan Liu⁴

¹School of Mechanics, Architecture and Civil Engineering, China University of Mining and Technology, Beijing 100083, China

²State Key Laboratory for Geomechanics and Deep Underground Engineering, China University of Mining and Technology, Beijing 100083, China

³School of Architecture and Civil Engineering, Guizhou University of Engineering Science, Guizhou, Bijie 551700, China

⁴Department of Metallurgy and Mineral Processing University of Zambia, P.O.Box 32379 Lusaka, Zambia

Received 2 June 2018; Accepted 19 September 2018

Abstract

Problems of large deformation of surrounding rock, such as large damage range and difficult support, are prominent during the period of gob-side entry driving excavation. Such problems seriously affect the safety and production efficiency in coal mines. To control the deformation of the surrounding rocks in the roadway, reduce supporting pressure, and determine a reasonable design for entry protection coal pillar, a numerical simulation study, theoretical analysis, and actual field measurement analysis were adopted under the engineering background of 7329 working face in Nantun Coal Mine in Jining, Shandong, China to analyze the stress distribution features and the deformation laws of the surrounding rock and the gob lateral supporting pressure distribution features under different coal pillar widths in the return airway of 7329 working face. Finally, on the basis of the combination of the three aforementioned methods, the optimal coal pillar width in a high-stress gob-side entry was proposed. Results show that the amplitude increasing extent in the vertical stress of the coal pillar is large under a small coal pillar width and exhibited linear increase. As the coal pillar width increases, the area of the elastic nuclear region also increases and the stress increasing extent tends to be stable without any apparent increasing trend. Gob-side entry wall deformation decreased with the increase in coal pillar width, whereas the deformation of solid coal wall shows an opposing trend; thus, the size range of a narrow coal pillar in the roadway was determined as 5-6 m. The width of roadway-protecting coal pillar is determined as 6 m through numerical simulation and theoretical analyses. The rationality of 6 m pillar is verified through an industrial test, which effectively solved the difficult support of gob-side entry and large deformation problems. The obtained conclusions could provide a certain reference for reasonable location selection of roadways under similar geological conditions.

Keywords: Width design, Numerical simulation, Stress distribution, Gob-side entry

1. Introduction

Coal is the main energy source in China, comprising 76% and 69% of primary energy source production and consumption, respectively. Within a considerably long time period, China will keep a coal-centered energy consumption structure. As important measures in constructing a conservation-minded society and implementing sustainable energy source strategies, reasonable utilization and use of coal resources, further improvement of coal resource recovery rate, and ecological environmental protection have become the main focus of research and development in the coal industry within China. Meanwhile, achieving roadway stability in gob-side entry driving process remains a problem in mining.

Gob-side entry driving is a technology for layout and maintenance of the coal mine gateway [1-6]. Specifically, a narrow coal pillar is retained at the gob side along the upper district sublevel for the driving gateways of the working face after the mining of the working face in the upper district sublevel becomes stable. Surrounding rock deformation laws of gob-side entry driving are apparently different from other

gateways mainly because of the properties of coal and rock masses surrounding the roadway and coal and the rock structure formed above the roadway after the mining of the working face in the upper district sublevel, causing high stress of the surrounding rocks in the gateways. Moreover, as the coal pillar is affected by dynamic pressure, the failure law is exceptionally complicated, which poses an enormous challenge to coal roadway anchor-pile support technology. In addition, the influence generated by mining of the adjacent working face on existing coal mine ventilation and secondary dynamic pressure of the haulage roadway results in repeated loading on the coal mine ventilation at the coal seam and haulage roadway, such that they suffer serious damage and heavy repair task. Therefore, reasonable determination of protective coal pillar width in the gob-side entry driving is of great importance in controlling roadway deformation and maintaining a favorable state.

As the mining depth increases, the width of the needed coal pillar in the district sublevel becomes increasingly greater if the coal pillar is used for protecting the mining roadway, which not only results in difficult roadway maintenance, high maintenance cost, and low coal recovery rate but also causes difficult adjacent coal seam mining due to the concentrated stress formed by the large coal pillar; these problems can easily induce disasters, such as rock burst, coal burst, and gas outburst [7-11]. The development

*E-mail address: wangjiong216@126.com

ISSN: 1791-2377 © 2018 Eastern Macedonia and Thrace Institute of Technology. All rights reserved.

doi:10.25103/jestr.114.07

of roadway protection technology using small coal pillars is effective in solving the aforementioned problems. With the progress of computer technology, research and manufacturing of new type of anchor bolt materials, and extension of coal pillar instability theory [12-14], researchers have conducted a large quantity of theoretical and practical studies on gob-side entry driving technology under high-stress condition and achieved many satisfying results. However, most of the existing studies have conducted optimized support design of the existing roadways but not taking entry protection coal pillar as the main study object. Moreover, most of the existing studies on gob-side entry driving have used a single method with complicated calculation, failing to combine numerical simulation analysis, theoretical calculation, and field practice in studying coal pillar width optimization problem.

On this basis, numerical simulation analysis, theoretical calculation, and field practice are combined in the present work to study the optimization design of coal pillar width in the high-stress gob-side entry, which provides a basis for maintaining stability of the high-stress gob-side entry.

2. State of the art

The retention of narrow coal pillar plays a remarkable role in surrounding rock stability in the gob-side entry, and many scholars have studied the reasonable position determination of the roadway excavation of a fully mechanized working face [15-16]. Bai et al. deemed that after mining of the working face in the upper district sublevel, a stress reduction region of a certain range existed at the coal edge (generally being 0-7 m), which constituted an advantageous condition for the gob-side entry layout; however, the focus was on research and development of a new type of supporting materials but little attention was given to the width design of entry protection coal pillar [7]. Li et al. analyzed several factors influencing gob-side entry driving position, such as main roof strata collapse and deformation features of immediate roof and coal mass, and determined the reasonable position of fully mechanized gob-side entry driving; however, the influence of lateral dynamic supporting pressure on the chain pillar was ignored [18]. Esterhuizen et al. inferred the estimation formula of coal pillar strength, considering potential influences of rock strength and wide-angle discontinuity on coal pillar strength [19]. Zhang et al. studied major deformation problems of surrounding rocks in the gob-side entry driving under unstable overlying strata and insisted that fracture, revolution, and slippage of main roof caused the major deformation of this type of surrounding rocks in roadways [20]. Chen et al. developed a strip coal pillar design approach, which was successfully applied to Daizhuang Coal Mine in China [21]. Although the aforementioned theoretical analyses can exert favorable guiding effects on chain pillar design, their calculation process is complicated and their results are strongly pertinent but not universal. Tan et al. considered in the pillar system of strip Wongawilli mining, some damaged or irregular pillars would become unstable under the coupling effect of mining pressure, ground water immersion and other unfavorable factors [22]. Zhang et al. proposed a new two-step gob-side entry driving technology, which, taking gangues as the aggregate, precasted the artificial wall for narrow coal pillar replacement [23]. Although they acquired good maintenance effect, the stability of this new material needed further

verification. Zhang et al. also proposed a prestressing combined support technology for gob-side entry driving in heading working face [24]. Gao et al. developed an equation for estimating the width of non-elastic zone in an inclined coal pillar, considering the plastic softening nature of coal and the coal seam pitch [25]. Zheng et al. studied stress field distribution laws in the entire gob-side entry driving process under different widths of entry protection coal pillar and proposed that two factors, namely, driving disturbance and advanced mining of the working face, should be considered to determine a reasonable coal pillar width [26]. However, insufficient concern was given to the change features of the displacement of the surrounding rocks in roadways.

With the progress of computer technology, numerical simulation software has been widely applied to the design of entry protection coal pillar in gob-side entry driving. Bai et al. stated that a yield pillar should release a large amount of energy and that rib bolting was necessary in controlling the pillar deformation and maintain the proper opening size [27]. Li et al. developed a numerical model using FLAC3D code for investigating two cases of yield pillar application in Chinese mines, in which double-yielding models were adopted for simulating gob materials [28]. Cheng et al. built a 3D simulation model using FLAC3D code for the design of coal pillars in an inclined thick coal seam [29]. In addition, as coal yield continuously increases, numerous scholars have conducted a large number of theoretical analyses of deformation failure mechanism and deformation control of gob-side entry and proposed large and small structural stability principles in fully mechanized gob-side entry driving and calculation formulas of lateral supporting pressure peak position. Using the previous theory, researchers have conducted in-depth studies and analyses of narrow coal pillar width and lateral supporting pressure peak position at gob side and achieved satisfying results [30-31]. However, the research methods are relatively singular, and theoretical analysis, numerical simulation, and field industrial test are not favorably combined. Moreover, the designed narrow coal pillar width at gob side has not generated a good effect on gob-side entry stability control in actual application.

Directing at the deficiencies of existing studies, theoretical analysis, numerical simulation, and field industrial test are combined to analyze the influence of gob-side coal pillar width on roadway stability on the precondition of a comprehensive consideration of the gob-side supporting stress distribution laws; the relationship of stress field distribution, displacement field distribution, and deformation of surrounding rocks in the roadway with coal pillar width; and the theoretical calculation of ultimate balance of narrow coal pillar width. Thus, a certain basis is provided for the stability of surrounding rocks in roadways under similar geological conditions.

The remainder of this study is organized as follows. Section 3 explains the engineering background and model establishment. Section 4 explains the numerical simulation, theoretical calculation results, and application to engineering practice. Section 5 draws the relevant conclusions.

3. Methodology

In the previous roadway driving process of Nantun Coal Mine in Jining, Shandong, China, the entry protection technology using large coal pillars was adopted; however, major deformation and serious damage already occurred on

the surrounding rocks in the roadway before recovering the working face and after the haulage roadway, which was not influenced by the driving process. Repeated artificial wall expansion and floor driving were needed to maintain normal use of the roadway. A major deformation with roof leakage and caving dangers occurred on the roof. Such serious roadway deformation and failure before recovering the working face considerably affected the safety and efficiency of production. The 7329 working face in Nantun Coal Mine was taken as the study object. Theoretical analysis, numerical simulation test, and field test were combined in this study to determine the width of entry protection coal pillar for controlling surrounding rock deformation in the roadway.

3.1 Engineering background

The 7329 working face of Nantun Coal Mine is located in Jining City, Shandong Province, China. The working face adjacent to 7329 has been finished, #3 coal seam is mainly mined, average coal seam thickness is 4 m, and burial depth is 300 m. The gob-side entry driving is needed in the return airway of 7329 working face to optimize the roadway layout and improve the recovery rate in the mining area. The planar layout of the test roadway is shown in Fig. 1.

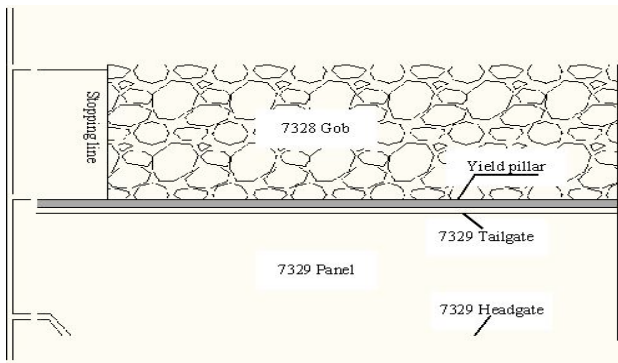


Fig. 1. Planar graph of roadway layout in 7329 working face

3.2 Numerical simulation analysis

Under the background of 7329 working face, a mining model under one-side gob condition is established. The width of entry protection coal pillar is determined by detecting stress change of roadway roof and floor during the stopping period.

3.2.1 Establishment of the numerical model

On the basis of the site geological conditions of the 7329 working face, FLAC3D numerical software is used to establish a 3D numerical simulation model of gob-side entry driving. As shown in Fig. 2, dimensions of the 3D numerical model are 320 m (length) × 250 m (width) × 170 m (height), and coal seam thickness is 4 m. Simulated burial depth is 350 m; a 4.5 MPa vertical uniformly distributed load is applied to the top of the model; and the load showing trapezoid distribution was applied in the horizontal direction, which is 0.5 times of that in the vertical direction. Moreover, horizontal displacement limiting boundary is adopted for the periphery of the model, whereas vertical displacement limiting boundary is adopted for the base. The physical and mechanical parameters of the rock mass of the model are shown in Table 1. During analog calculation, a double-yielding model was used for the caving zone, and Mohr-Coulomb strength criterion is used for other rock masses [32]. Anchor-pile support technology is used for the simulated roadway support. The roadway supporting intensity has an important effect on narrow coal pillar stability. However, this study centers on the determination of narrow coal pillar width; thus, the unified supporting intensity is used for anchor-pile support in this simulation by combining the actual situation of roadway anchor-pile support system in the coal mine.

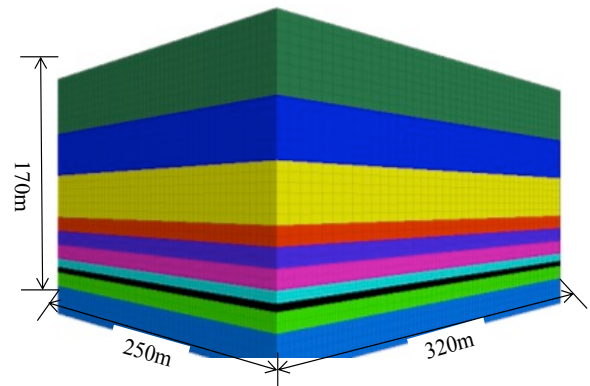


Fig. 2. 3D numerical model

Table 1. Strata lithology and mechanical properties

Lithology	Thickness (m)	Density (kg/m ³)	Bulk modulus (GPa)	Shear modulus (GPa)	Cohesive force (MPa)	Tensile strength (MPa)	Frictional angle (°)
Medium sandstone	20	2,520	18.3	11.5	1.2	3.96	41
Claystone	28	2,300	15.2	6.25	0.1	1.55	31
Medium sandstone	8	2,520	18.3	11.5	1.2	3.96	41
Claystone	4	2,300	15.2	6.25	0.1	2.8	31
Siltstone	8	2,530	13.4	7.6	1.4	1.85	37
Medium sandstone	28	2,520	18.3	11.5	1.2	3.96	41
Siltstone	8	2,530	13.4	7.6	1.4	1.85	37
#3 Coal	8	1,350	10.5	6.5	1.2	0.5	23
Fine sandstone	4	2,530	13.4	7.6	1.4	4.0	37
Medium sandstone	12	2,520	18.3	11.5	1.2	3.96	41
Mudstone	12	2,340	9.8	7.1	0.5	3.0	39
Fault	1	2,000	0.01	0.0035	0.001	0.2	5
Caving zone	8	1,700	0.0199	0.001	0.001	0	30

3.2.2 Simulation and monitoring scheme

On the basis of the design requirements, narrow coal pillar width is set as 3, 4, 5, 6, 7, and 8 m to study stress distribution features and deformation laws of surrounding rocks in the roadway under different coal pillar widths. Two monitoring lines are arranged at the side of the designed laneway to record the stress and displacement change during mining. Monitoring points are also arranged at the roadway roof, floor, and two walls to record the required stress and displacement data, as shown in Fig. 3.

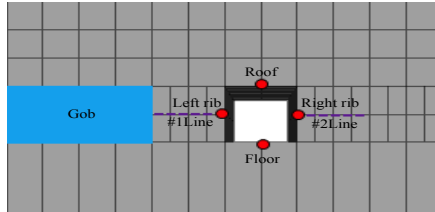


Fig. 3. Monitoring scheme

4 Test results and analysis

4.1 Experimental settings

The supporting pressure distributions of the surrounding rock under different narrow coal pillar widths are shown in Fig. 4. The stress distribution state of the surrounding rocks in the roadway varies when different coal pillar widths are retained in the gob-side entry driving. The vertical stresses at the roadway roof and floor are under low-stress states, and the stresses are basically kept identical. Stress concentration degree is high at the solid wall side, and they slightly vary under different coal pillar widths. Considerable differences exist in the effects of the different gob-side coal pillar widths. As the coal pillar width continuously increases, the elastic stability region in the coal pillar is enlarged, accompanied by enhanced bearing capacity.

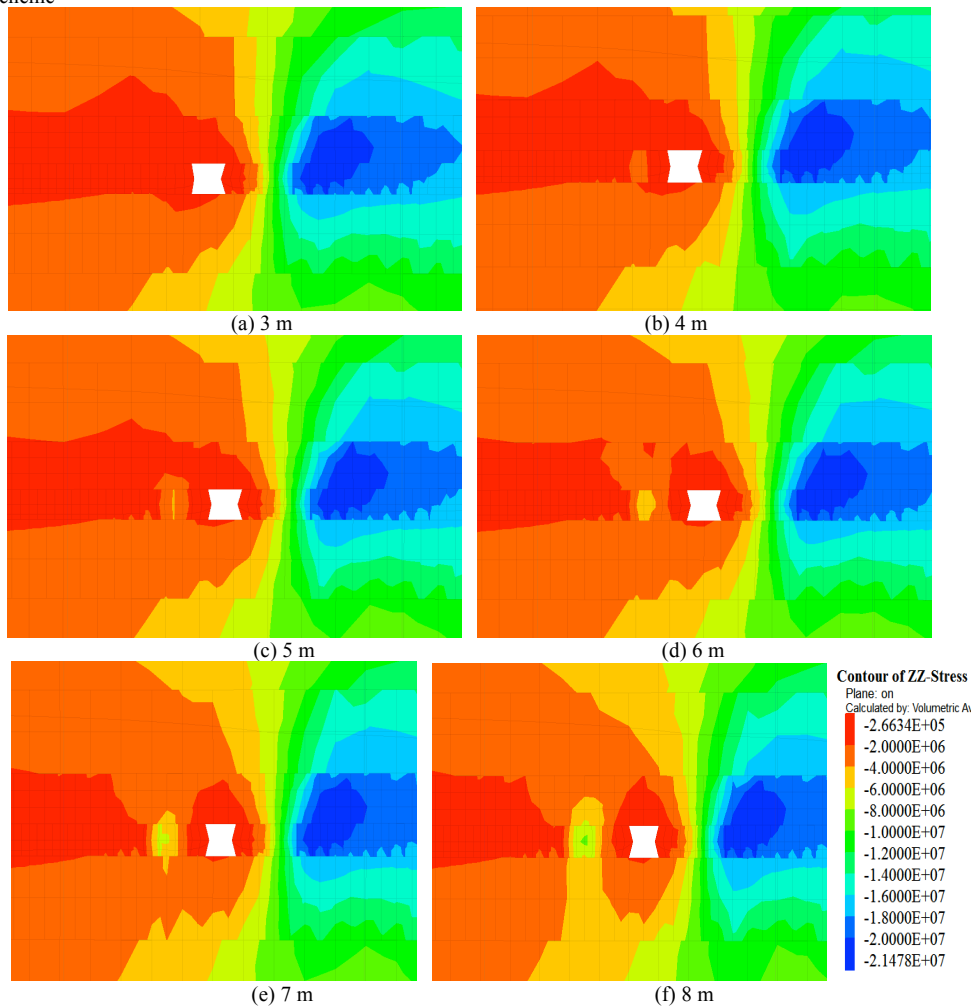


Fig. 4. Stress distributions of the surrounding rocks under different coal pillar widths

Vertical stress and stress peak in the narrow coal pillar are compared to analyze the influence of coal pillar width on the stability of the surrounding rocks in the roadway. Fig. 5 shows the stress distribution features of the surrounding rocks under different coal pillar widths, and Table 2 shows the varying distributions of peak value with change in coal pillar width. As shown in Fig. 5, the effect of coal pillar width is considerable and the peak region inside the coal pillar is gradually enlarged when its width increases from 3 m to 8 m. When the coal pillar width is within 3-4 m, the narrow coal pillar is under plastic failure state, the stress peaks of the coal pillar are 1.9 MPa and 2.5 MPa, elastic

nuclear region does not exist inside the coal pillar, and the bearing capacity is weak. When the coal pillar width is within 4-5 m, the vertical stress increases and stress peak reaches to 4.4 MPa and 5.1 MPa. The increase in coal pillar width causes its bearing capacity to strengthen and bear forces from the overlying strata. When the coal pillar width is within 6-8 m, the elastic core region inside the coal pillar is enlarged and stress peaks are 5.1, 6.17, and 8.02 MPa. Finally, when the coal pillar width is within 6-8 m, elastic region inside the coal pillar is remarkably enlarged and stress concentration occurs.

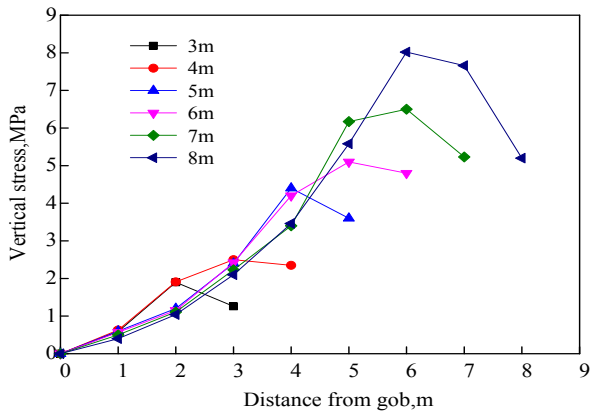


Fig. 5. Vertical stress distributions under different coal pillar widths

Table 2. Stress peak change under different coal pillar widths

Coal pillar width (m)	3	4	5	6	7	8
Peak stress inside the coal pillar (MPa)	1.9	2.5	4.4	5.1	6.17	8.02

As shown in Table 2, the amplitude increases in vertical stress peak values greatly vary under different coal pillar widths. When the coal pillar width is within 4 m, the stress peak increases by 0.6 MPa with 31.6% increasing extent. Within 4-5 m, the vertical stress peak abruptly increases by 1.9 MPa with 31.6% increasing extent. Within 5-6 m, the vertical stress increases by 0.7 MPa with 31.6% increasing extent. Stress amplitude increases are 27.4% and 23.1% within 6-7 m and 7-8 m, respectively. Therefore, amplitude increase in coal pillar vertical stress is large under a small coal pillar width, which denotes linear growth. As the coal pillar width increases, the area of the elastic nuclear region is enlarged and the stress amplitude increase tends to be stable without any apparent increasing trend. In sum, stress concentration does not exist within 6 m, under which vertical stress is considerably lower than primary rock stress. The coal pillar is under plastic failure state with weak bearing capacity. When the coal pillar width is within 5-6 m,

the elastic nuclear regional distribution is relatively uniform in the coal pillar and stress concentration does not exist inside the coal pillar. However, the coal pillar has bearing capacity, and stress is basically identical with primary rock stress. Within 7-8 m, the stress peak is located in the middle of the coal pillar, the stress is higher than the primary rock stress, and the influence scope of the stress peak is large. Therefore, in view of the effect of coal pillar width and stress distribution features of the surrounding rocks, the reasonable coal pillar width is within 5-6 m.

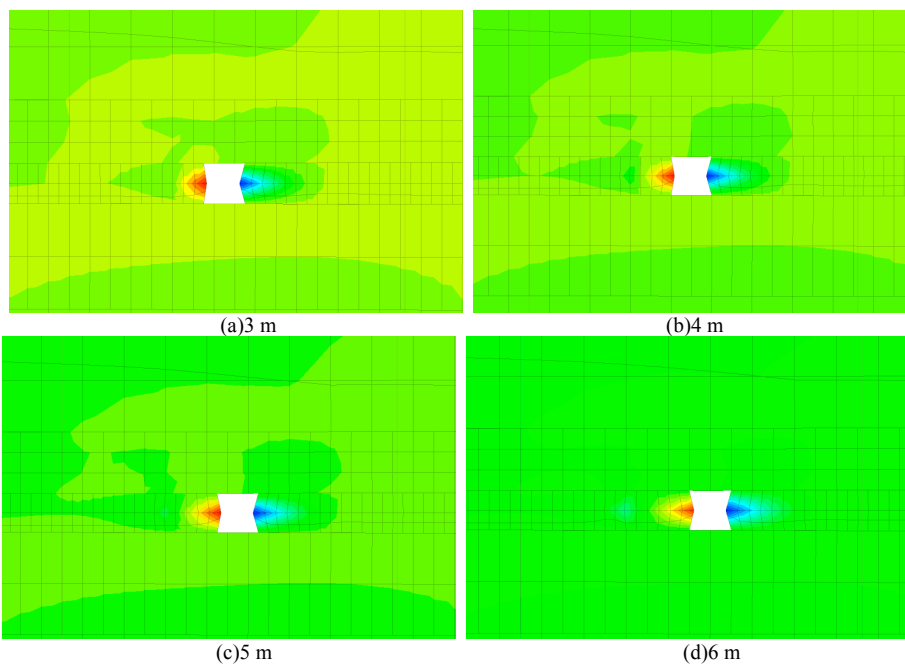
4.2 Surrounding rock deformation laws in gob-side entry driving under different coal pillar widths

Roadway deformations under different narrow coal pillar widths are shown in Fig. 6. Gob-side entry driving under different coal pillar widths can generate displacement at the gob side and inside the roadway. Moreover, the deformation of the gob-side entry driving is greater than that at the solid coal side. As the coal pillar width increases, the deformation of the gob-side entry driving decreases and the wall deformation in the solid coal side increases.

As shown in Fig. 7, when the coal pillar width is within 3-5 m, the horizontal displacement peak value of the coal pillar toward the gob side increases from 55 mm to 100 mm. Within 5-7 m, the horizontal displacement peak value toward the gob side remarkably reduces from 100 mm to 54 mm, with reduction amplitude reaching 46%. When the coal pillar width is greater than 7 m, the horizontal displacement reduces slowly and it reduces to 49 mm under 8-m condition.

Horizontal displacement peak value toward the roadway side gradually reduces with the increase in coal pillar width. The displacement peak value shows fast linear growth from 64 mm to 90 mm (amplitude increase is 41%) when the coal pillar width is within 3-4 m; whereas, it increases from 89 mm to 115 mm (amplitude increase is 22.6%) within 4-7 m. The increase apparently slows down compared with the last range. When the coal pillar width is greater than 7 m, the horizontal displacement peak value increases slowly.

In sum, the coal pillar width should be controlled within 5-7 m.



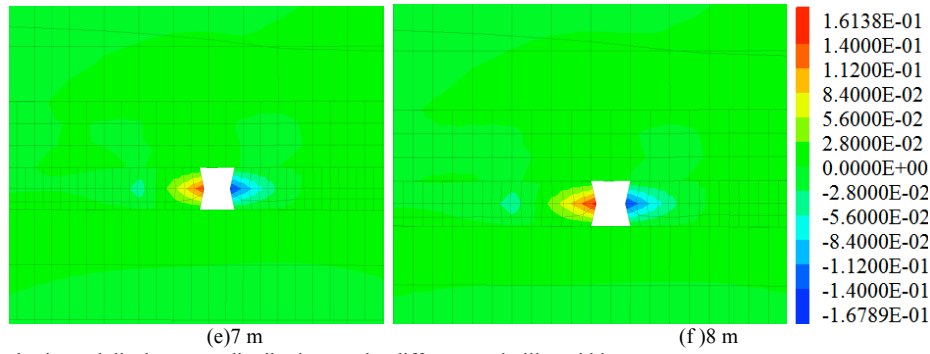


Fig. 6. Roadway horizontal displacement distributions under different coal pillar widths

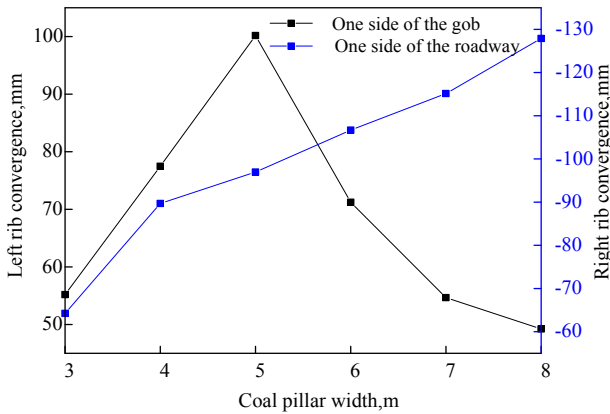


Fig. 7. Horizontal displacement curves of the coal pillar toward the gob side and roadway under different coal pillar widths

The deformation law of the surrounding rocks in roadways under different coal pillar widths is shown in Fig. 8. The deformation law of roadway roof, floor, and two walls varies under different coal pillar widths. Roadway roof sinkage has a positive correlation with the coal pillar width. When the coal pillar width is within 3-4 m, the roof sinkage is small but increases with the coal pillar width from 100 mm to 112 mm; the amplitude increase is 12%, which is small. When the coal pillar width is within 5-7 m, roof sinkage increases from 120 mm to 135 mm, with 12.5% amplitude increase. When the coal pillar width is within 7-8 m, roof sinkage has a relatively small increase from 135 mm to 140 mm and roof deformation is basically stable. Coal pillar width has a minor influence on the heaving floor because it remains unchanged with the increase in coal pillar width.

Wall displacement quantity at the solid coal side increases with the coal pillar width. When the coal pillar width is within 3-5 m, the wall displacement quantity is small, increasing from 115 mm to 121 mm, and the amplitude increase is also small. Under the 6-m condition, the wall displacement increases considerably, reaching 159 mm; however, the displacement quantity is not that large. Within 6-8 m, the wall displacement at the solid coal side continues to increase from 159 mm to 163 mm. After the coal pillar width reaches 6 m, the amplitude increase in the wall displacement is small, with no apparent change.

Gob-side wall displacement is apparently smaller than that at the solid coal side. When the coal pillar width is within 3-5 m, the wall displacement increases from 48 mm to 77 mm, with a 60% amplitude increase; however, the displacement quantity is small. Wall displacement quantity increases from 77 mm to 96 mm under 5-7-m condition. When the coal pillar width is greater than 7 m, increase in

wall displacement quantity has minimal changes and maintains stability.

Therefore, the coal pillar width has a great influence on roof sinkage and solid coal wall in the gob-side entry driving but a relatively small influence on the heaving floor. On the basis of the analysis on the deformation of the surrounding rocks in the roadway, the reasonable coal pillar width is 5-7 m.

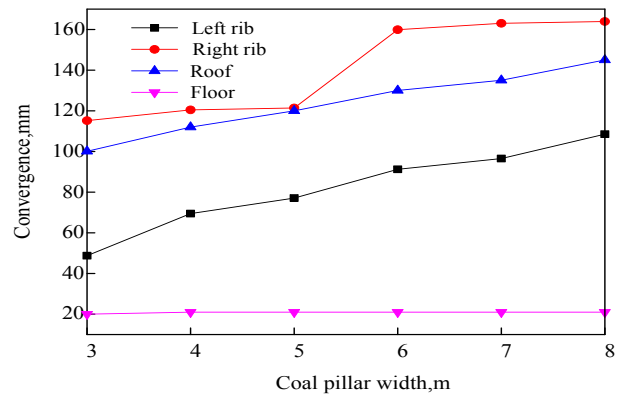


Fig. 8. Relationship between coal pillar width and deformation of the surrounding rocks in the roadway

4.3 Theoretical analysis on the reasonable coal pillar width

Coal pillar stability is the key in maintaining the stability of gob-side entry driving. After the working face of the upper district sublevel is mined, the main strata of the overlying roof are fractured above the coal body. Stress reduction zone, stress increase region, and the original rock stress area comprises the coal body in the order from the coal wall to the deep part. The smallest coal pillar width should be obtained to ensure that the roadway is in the stress reduction region; however, if the coal pillar is extremely narrow, serious crushing of the coal mass occurs with weak bearing capacity, which is contrary to anchor-pile support and gob isolation. Therefore, a reasonable coal pillar width exists, which not only allows the coal pillar to be in the stress reduction region nearby the coal wall and reduce coal resource loss but also ensures high bearing capacity of the coal pillar and maintains stability of the surrounding rocks in the roadway.

On the basis of failure degree, crack distribution, and bearing capacity of the coal seam structure, the coal mass at the external side of the gob can be divided into non-intact region (Region A), relatively intact region (Region B), and intact region (Region C) along the inclined direction, as shown in Fig. 10. The coal mass structure in Region A obtains serious failure without crack development, whereas

that in Region B is not damaged without crack development. Both structures have bearing capacity. The gob-side entry should be arranged inside Region B or C to prevent secondary disasters, such as spontaneous combustion of the residual coal in the gob and gas outbursts. Thus, the width of region A is an important basis for determining the position of gob-side entry.

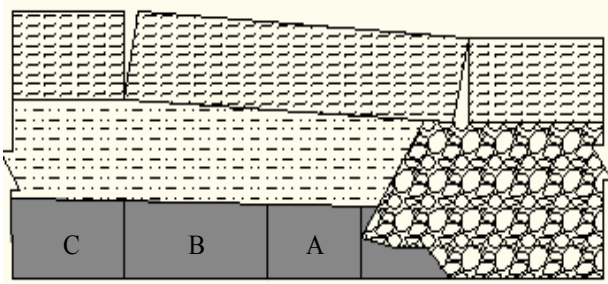


Fig. 9. Intactness division of lateral coal mass in the working face in the upper district sublevel

The two sides of the entry protection coal pillar in the gob-side entry driving in the 7932 working face are the 7328 working face gob and return airway of the 7329 working face. On the basis of the ultimate balance theory, the calculation of the coal pillar width is shown in Eq. (1). The calculation chart is shown in Fig. 10 [16].

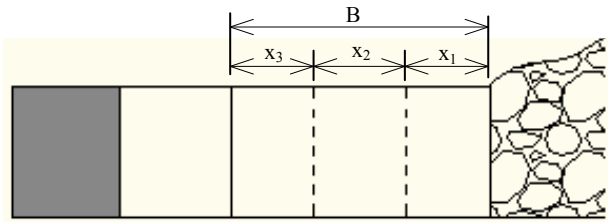


Fig. 10. Calculation chart of the coal pillar width

$$B = X_1 + X_2 + X_3, \quad (1)$$

where B is the coal pillar width, m; X_1 is the plastic zone width generated in the gob-side coal mass after the mining of the working face, m, and its value is calculated in Eq. (2); X_3 is the effective length of the anchor bolt, 1.3 m; and X_2 is the coal pillar stability coefficient, which is increased on the basis of the large coal seam thickness and is calculated on the basis of $(X_1 + X_3)$ (30%–50%).

$$X_1 = \frac{mA}{2 \tan \varphi_0} \ln \left[\frac{K\gamma H + \frac{C_0}{\tan \varphi_0}}{\frac{C}{\tan \varphi_0} + \frac{p_z}{A}} \right] \quad (2)$$

where m is the coal seam mining thickness, 4 m; A is the lateral pressure coefficient, $A = \frac{\mu}{1-\mu}$, where the Poisson's ratio is $\mu = 0.18$ and $A = 0.22$; φ_0 is the internal frictional angle at the coal seam interface, 25° ; C_0 is the cohesive force of the coal seam interface, 1.3 MPa; K is the stress concentration coefficient, 2; γ is the average strata bulk weight, 25 kN/m^3 ; H is the roadway burial depth, 350 m; and p_z is the supporting resistance provided by the anchor bolt to the coal wall, 0.3 MPa.

When the aforementioned values are substituted into Eqs. (1) and (2), $X_1 = 2.7 \text{ m}$ and $X_2 = 1.3\text{-}2 \text{ m}$; thus, $B = 5.2\text{-}6.11 \text{ m}$. The coal pillar width is 6 m.

Rupture, revolution, and slippage of the overlying strata, especially the main roof, are aggravated during the mining of the working face, and the caused dynamic pressure load is mainly from the coal mass in the front of the working face (solid coal wall in the gob-side entry), coal gangue, and narrow coal pillar in the gob. Coal mass and coal gangue have great bearing capacities, whereas the coal pillar has weak bearing capacity; thus, the "large structure" formed due to rupture, revolution, and slippage of the overlying strata is a key factor in deciding the narrow coal pillar stability in the gob-side entry. The crushing status of the coal mass of the coal pillar is aggravated. As the overlying strata become gradually stable, the coal mass deformation in the coal pillar gradually tends to be stable. Gob lateral supporting pressure is divided into stress reduction region, stress increase region, and primary rock stress region. When the roadway is in the stress reduction region, the surrounding rock stress state of the narrow coal pillar in the gob-side entry driving is greatly improved, the roadway deformation is reduced, and the surrounding rock stability is good. Therefore, the roadway is arranged in the stress reduction region. After the mining of 7328 working face, the lateral supporting pressure distribution laws obtained through field measurement are shown in Fig. 11.

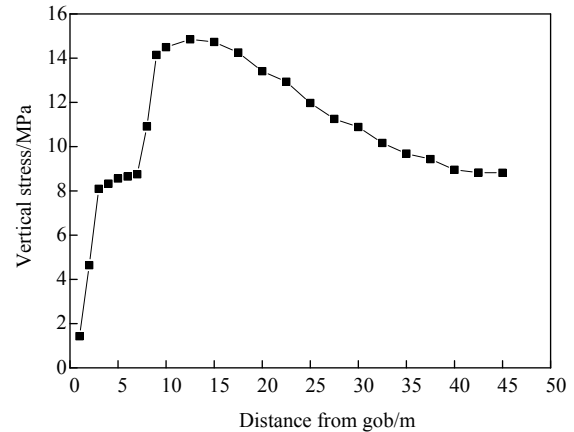


Fig. 11. Lateral supporting pressure distribution law curve

Fig. 11 shows that the vertical stress changes with the distance from the gob edge after the mining of the upper working face. Within 1-3 m distance, the vertical stress abruptly increases from 1.4 MPa to 7.3 MPa. The amplitude increase in the vertical stress is not large within 3-7 m and smaller than that within 1-3m, and the vertical stress is lower than the primary rock stress. The vertical stress rapidly increases within 8-15 m from 11.2 MPa to 14.7 MPa. The vertical stress reaches the peak value at 15 m, and the stress concentration factor is 1.68. The vertical stress gradually reduces within 15-40 m and reaches stability after 40 m, thereby returning to the original rock stress. Therefore, lateral supporting pressure is in the stress reduction region within 0-7 m, in the stress increase region within 8-40 m, and in the primary rock stress region after 40 m. Gob-side entry should be arranged in the stress reduction region or the primary rock stress region because arranging it in the primary rock stress region can cause an enormous waste of coal resources. Therefore, the coal pillar width should be controlled within 0-7 m in the gob-side entry.

4.4 Theoretical analysis on the reasonable coal pillar width

Combined with theoretical analysis and numerical simulation calculation, the width of the narrow coal pillar is 5-7 m on the basis of fully considering the position layout of the gob-side entry. A certain area of stable elastic nucleus exists inside the coal pillar under this width. The deformation quantity of the surrounding rocks in the roadway is also small. Finally, in view of the coal resource saving principles, the reasonable coal pillar width in the gob-side entry driving is determined as 6 m.

4.5 Field industrial test

On the basis of the already designed coal pillar, the coal pillar width was set as 6 m. The supporting scheme shown in Fig. 12 was adopted for the return airway of the 7329 working face. The screw-thread steel anchor bolts at the wall were 20 mm × 2,400 mm, and their inter-row spacing was 1,200 mm × 1,200 mm. The size of the roof anchor cables was 22 mm × 5,000 mm, which were arranged vertically to the roof. Their inter-row spacing was 12,000 mm × 2,000 mm, and they were connected using W steel bolts.

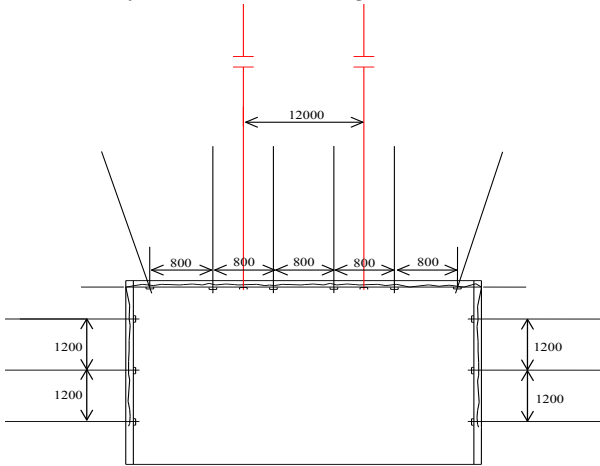


Fig. 12. Schematic of the return airway support in the 7329 working face (unit: mm)

A monitoring section was set every other 150 m to monitor the deformation quantity of the surrounding rocks in the roadway and the load-carrying status of supporting members during roadway excavation. Figs. 13 and 15 show the monitoring curves of the roadway surface displacement and the load bearing of anchor bolts and cables.

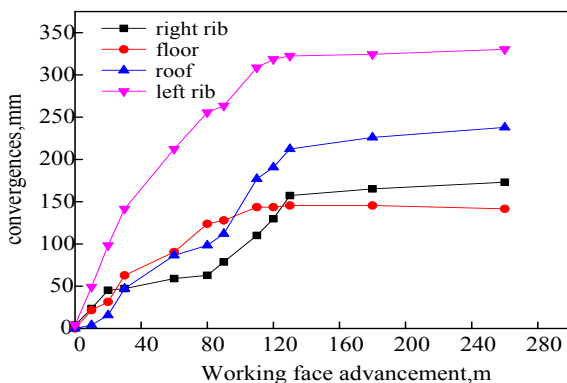


Fig. 13. Roadway surface displacement curves

As shown in Fig. 13, when the monitoring section is 0-90 m away from the open-off cut during the mining of the

working face, the roadway surface displacement rate is large, where the deformation rate of the surrounding rock at the gob-side wall reaches 9 mm/m, with the advancement of the working face. As the working face continues to advance, the surrounding rock deformation slowly increases. After the monitoring section is more than 120 m away from the open-off cut, the surrounding rock deformation tends to be stable and the deformation speed of the gob-side entry is only 0.9 mm/m. The maximum values of the roof sinkage and heaving floor sinkage are 254 mm and 145 mm, respectively. The maximum displacement values inside the solid wall and inside the gob-side wall are 173 mm and 320 mm, respectively.

Fig. 14 shows that the loads from the anchor bolts and anchor cables grow rapidly within the 0-30 m mining range. When the monitoring section is 90 m away from the open-off cut, the load bearing of the anchor bolts and anchor cables tends to be stable. The solid wall > roof > gob-side wall features are present, indicating that the solid coal wall is the main body bearing the overlying strata during the gob-side entry driving. Maximum loads from the anchor bolts and anchor cables are 121 kN and 184 kN, respectively, after becoming stable. Both loads are within their yield limits, and sufficient margin is reserved during the mining period. Field monitoring results indicate that the retained 6 m coal pillar width is reasonable.

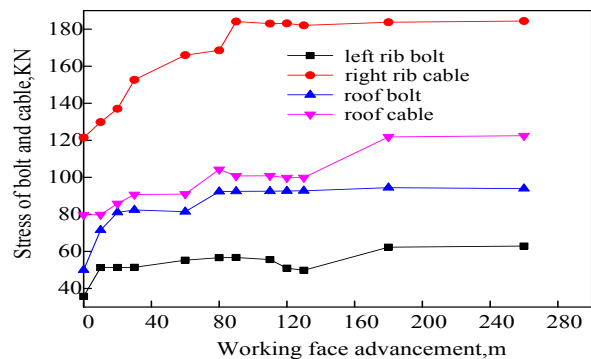


Fig. 14. Load-bearing monitoring curves of anchor bolts and anchor cables

5 Conclusions

Theoretical analysis, 3D numerical simulation, and field test are combined in this study to obtain reasonable narrow coal pillar width in the gob-side entry driving. The main conclusions are obtained as follows.

(1) On the basis of the lateral supporting pressure distribution law obtained through the actual measurement, the gob-side entry driving position should be selected within the stress reduction region or primary rock stress region. Arranging the roadway in the primary rock stress region will result in coal resource wastage; thus, it should be arranged in the stress reduction region.

(2) The coal pillar width is positively correlated with the vertical stress. When the coal pillar width is small (0-5m), plastic fracture occurs on the coal pillar, thereby causing degradation of its bearing capacity and elastic nucleus is not present. Within 5-6 m, the elastic core region is uniformly distributed in the coal pillar, which has a certain bearing capacity without any stress concentration. When the coal pillar width is greater than 6 m, the coal pillar stress peak value is greater than the primary rock stress. The coal pillar width has considerable influence on the displacement

quantities of the two roadway walls and roof sinkage but only has minor influence on the heaving floor.

(3) A reasonable narrow coal pillar width in the gob-side entry driving is determined as 6 m, considering the supporting stress distribution laws of the district sublevel gob-side; the relationship of stress field distribution, displacement field distribution, and the deformation of the surrounding rocks in the roadway with coal pillar width; and the theoretical calculation of the narrow coal pillar width balance.

Therefore, the coal pillar width in the gob-side entry driving proposed in this study has been successfully applied in practical engineering, which has improved the surrounding rock environment in the roadway, reasonably controlled deformation of gob-side entry, reduced roadway

maintenance expense, improved safe coal mining environment, and laid a foundation for the stability control of the surrounding rocks in the roadway under similar geological conditions. However, the reasonability of the gob parameters used in the numerical simulation process is not verified because these parameters may have a certain deviation from the actual parameters. Therefore, inversion of the selected gob parameters should be conducted in the future to ensure parameter reliability.

This is an Open Access article distributed under the terms of the Creative Commons Attribution Licence



References

1. Li W., Bai J., Peng S., et al, "Numerical modeling for yield pillar design: a case study". *Rock Mechanics & Rock Engineering*, 48(1), 2015, pp.305-318.
2. Zhang G. C., He F L, Jia H G, et al, "Analysis of gateroad stability in relation to yield pillar size: a case study". *Rock Mechanics & Rock Engineering*, 50(5), 2017, pp.1-16.
3. Jaiswal A., Shrivastva B. K., "Numerical simulation of coal pillar strength". *International Journal of Rock Mechanics & Mining Sciences*, 46(4), 2009, pp.779-788.
4. Shabanimashcool M., Li C. C., "Numerical modelling of longwall mining and stability analysis of the gates in a coal mine". *International Journal of Rock Mechanics & Mining Sciences*, 51(4), 2012, pp.24-34.
5. Jiang L., Sainoki A., Mitri H. S., et al, "Influence of fracture-induced weakening on coal mine gateroad stability". *International Journal of Rock Mechanics & Mining Sciences*, 88, 2016, pp.307-317.
6. Hou C. J., LI X. H., "Stability principle of big and small structures of rock surrounding roadway driven along goaf in fully mechanized top coal caving face". *Journal of China Coal Society*, 26(1), 2001, pp.1-7..
7. Shen B T, "Coal mine roadway stability in soft rock: a case study". *Rock Mechanics & Rock Engineering*, 47(6), 2014, pp.2225-2238.
8. Zhang Z., Shimada H., Sciubba E., "Numerical study on the effectiveness of grouting reinforcement on the large heaving floor of the deep retained goaf-side gateroad: a case study in China". *Energies*, 11(4),2018,pp.1001.
9. Yu B., Zhang Z., Kuang T., et al, "Stress changes and deformation monitoring of longwall coal pillars located in weak ground". *Rock Mechanics & Rock Engineering*, 49(8), 2016,pp.3293-3305..
10. Najafi M., Jalali S. E., Bafghi A. R. Y., et al, "Prediction of the confidence interval for stability analysis of chain pillars in coal mines". *Safety Science*, 49(5), 2011,pp.651-657.
11. Mahdevari S., Shahriar K., Sharifzadeh M., et al, "Assessment of failure mechanisms in deep longwall faces based on mining-induced seismicity". *Arabian Journal of Geosciences*, 9(18), 2016, pp.709.
12. Li L., Bai J. B., XU Ying, et al., "Research on rock control of roadway with complex roof driven along goaf". *Journal of Mining & Safety Engineering*, 28(3), 2011, pp. 376-382
13. Peng L. J., Zhang D. F., Guo Z. B.,et al, "Numerical analysis of thick coal seam small pillar along gob roadway and its application". *Rock and Soil Mechanics*, 34(2), 2013, pp.3609-3617.
14. Bai J. B., Wang W. J., Hou C. J.,et al, "Control mechanism and support technique about gateway driven along goaf in fully mechanized top coal caving face". *Journal of China Coal Society*, 25(5), 2000, pp.478-481.
15. Li X. H., Zhang N., Hou C. J., "Rational position determination of roadway driving along next goaf for fully mechanized top coal caving mining". *Journal of China University of Mining and Technology*, 29(2), 2000, pp.186-189..
16. Esterhuizen G. S., Dolinar D. R., Ellenberger J. L., "Pillar strength in underground stone mines in the United States". *International Journal of Rock Mechanics & Mining Sciences*, 48(1), 2011, pp.42-50.
17. Zhang Y., Wan Z. J., Li F. C., et al, "Large deformation mechanism of roadway driving along goaf under unstable overlying rock strata". *Journal of Mining and Safety Engineering*, 29(4), 2012, pp.451-458.
18. Chen S., Wang H., Wang H., et al, "Strip coal pillar design based on estimated surface subsidence in Eastern China". *Rock Mechanics & Rock Engineering*, 49(9), 2016, pp.1-10..
19. Yu B., Zhang Z., Kuang T., et al, "Stress changes and deformation monitoring of longwall coal pillars located in weak ground". *Rock Mechanics & Rock Engineering*, 49(8), 2016, pp.3293-3305.
20. Zhang D. S., Wang H. S., Ma L. Q., "Two-step gob-side entry driving technology of pre-build artificial side substitute for narrow coal pillar". *Journal of China Coal Society*, 35(10), 2010, pp.1589-1593.
21. Zhang N., Li X. H., Gao M. S., "Pretension support of roadway driven along next gob and heading adjacent advancing coal face and its application". *Chinese Journal of Rock Mechanics and Engineering*, 23(12), 2004, pp.2100-2105.
22. Tan Y., Guo W. B, Bai E. H, Yan H., "Overburden failure induced by instability of coal pillar in strip Wongawilli mining". *Journal of China Coal Society*, 42(7), 2017, pp.1656-1662.
23. Zheng X.G, Yao Z.G, Zhang N., "Stress distribution of coal pillar with gob-side entry driving in the process of excavation and mining". *Journal of Mining and Safety Engineering*, 29(4), 2012, pp. 459-465.
24. Bai J., Hou C., Huang H., "Numerical simulation study on stability of narrow coal pillar of roadway driving along goaf". *Chinese Journal of Rock Mechanics & Engineering*, 23(20), 2004, pp.3475-3479.
25. Li W., Bai J., Peng S., et al, "Numerical modeling for yield pillar design: a case study". *Rock Mechanics & Rock Engineering*, 48(1), 2015, pp.305-318.
26. Cheng Y. M., Wang J. A., Xie G. X., et al, "Three-dimensional analysis of coal barrier pillars in tailgate area adjacent to the fully mechanized top caving mining face". *International Journal of Rock Mechanics & Mining Sciences*, 47(8), 2010, pp.1372-1383.
27. Li X. H., Zhang N. G., Hou C. J., "Rational position determination of roadway driving along next goaf for fully mechanized top coal caving mining". *Journal of China University of Mining and Technology*, 29(2), 2000, pp.186-189.
28. Xie G. X, Yang K., Liu Q. M., "Study on distribution laws of stress in inclined coal pillar for fully-mechanized top-coal caving face". *Chinese Journal of Rock Mechanics and Engineering*, 25(3), 2006, pp.545-549.
29. Wu Q. S., "Study on the law mining stress evolution and fault activation under the influence of normal fault". *Acta Geodynamica Et Geomaterialia*, 14(3), 2017, pp.357-369.